

Diffusion on fractals with singular waiting-time distribution

Harald Harder and Shlomo Havlin

*Department of Physics, Bar-Ilan University, Ramat-Gan, Israel
and Fakultät für Physik, Universität Konstanz, D-7750 Konstanz, Federal Republic of Germany*

Armin Bunde

Fakultät für Physik, Universität Konstanz, D-7750 Konstanz, Federal Republic of Germany

(Received 23 March 1987)

We study diffusion in lattices of arbitrary dimensions with a power-law distribution of waiting times τ , $P(\tau) \sim \tau^{\alpha-2}$, $\alpha < 1$, $\tau \geq 1$. Using general scaling arguments we find that the asymptotic behavior of the mean-square displacement of a random walker is given by $\langle r^2 \rangle \sim t^{2/\bar{d}_w}$, where $\bar{d}_w = d_w$ for $\alpha < 0$ and $\bar{d}_w = d_w \{1 + d_s \alpha / [2(1-\alpha)]\}$ for $0 \leq \alpha < 1$ and $d_s \leq 2$. Here d_w is the (conventional) diffusion exponent for constant waiting times and d_s is the fracton dimension of the substrate. Our expression for \bar{d}_w is general and holds for Euclidean lattices as well as for random and deterministic fractals. We have also investigated scaling properties of the distribution function $\bar{P}(l, t)$ and the corresponding moments $\langle l^q \rangle$, where l is the chemical distance the walker traveled in time t . To test our theoretical expressions we have performed extensive computer simulations on the incipient percolation cluster in $d=2$, using the exact enumeration method. The numerical results agree well with the theoretical predictions.

I. INTRODUCTION

In recent years, the problem of anomalous diffusion in random media has been investigated extensively.¹⁻⁷ In general, laws of diffusion in random systems have been characterized by power-law relations of the form

$$\langle r^2 \rangle \sim t^{2/d_w}, \quad (1)$$

where $\langle r^2 \rangle$ is the mean-square displacement of a random walker in the system and t is the time. In uniform lattices $d_w = 2$ and (1) reduces to Fick's law of diffusion. For random systems, d_w can accept values larger than 2. This anomalous diffusion occurs in self-similar random structures, e.g., in percolation clusters within the correlation length,² or in Euclidean systems with singular distributions of hopping rates or waiting times.^{7,8} While the behavior of d_w for each of both types of disorder is quite well understood, much less is known about random media where both types of disorder are present. Such systems are, for example, percolation systems with singular distributions of hopping rates or waiting times. Percolation systems with power-law distributions of hopping rates are relevant for describing transport in continuum percolation (random-void model).⁹⁻¹¹ In this case, exact analytical expressions for d_w are not known, but upper and lower bounds for d_w have been derived.⁹⁻¹¹ For percolation systems with a power-law distribution of waiting times τ ,

$$P(\tau) \sim \tau^{\alpha-2}, \quad \alpha < 1, \quad \tau \geq 1 \quad (2)$$

rigorous results have not been derived. In previous calculations, either approximative methods were used, such as the continuous-time random-walk approximation,¹² or deterministic fractals were considered, where renormalization-group approaches have been performed.¹³

In this paper we concentrate on the general problem of diffusion in Euclidean or fractal networks, with the waiting-time distribution (2). Using general scaling arguments we derive the following result for the transport exponent \bar{d}_w :

$$\bar{d}_w = \begin{cases} d_w, & -\infty < \alpha \leq 0 \\ d_w \left[1 + \frac{d_s}{2} \frac{\alpha}{1-\alpha} \right], & 0 < \alpha < 1, \quad d_s < 2 \\ d_w / (1-\alpha), & 0 < \alpha < 1, \quad d_s \geq 2 \end{cases} \quad (3)$$

where $d_w \equiv \bar{d}_w(-\infty)$ is the transport exponent for constant waiting times, and d_s is the fracton dimension. We believe that (3) is rigorous and holds for arbitrary dimensions d , including fractals. For special cases (Euclidean lattices and deterministic fractals) (3) reduces to the established results.^{7,8,13,14} To show explicitly that (3) holds also for *random* fractals we have performed extensive computer simulations of random walks on the incipient infinite percolation cluster in $d=2$ for several values of α . Our results support strongly the validity of (3).

In addition, we have considered the distribution function $\bar{P}(l, t)$ as well as the corresponding moments of the random walk on percolation clusters. We have found numerically that the scaling form for $\bar{P}(l, t)$ recently suggested by Havlin *et al.*¹⁵ for constant waiting times can be used successfully also to describe systems with waiting time distributions. In particular, the moments $\langle l^q(t) \rangle$ for $-\infty < q < +\infty$ can be described by the exponents d_l and d_s only.

II. THE DIFFUSION EXPONENT

After N steps of the random walker, the elapsed time t

is given by

$$t = N\bar{t}, \quad (4)$$

where \bar{t} is the average time the walker stays in one site. Since the mean-square displacement $\langle r^2 \rangle$ as a function of N steps of the random walker does not depend on how long the walker has to wait in a given site before he can jump, it scales as for constant waiting times, i.e.,

$$\langle r^2 \rangle \sim N^{2/d_w}. \quad (5)$$

For a distribution of waiting times, \bar{t} depends on N . From the number S of distinct visited sites we can evaluate \bar{t} ,

$$\bar{t} = \frac{1}{S} \sum_{i=1}^S \tau_i = \int_1^{\tau_{\max}} d\tau \tau P(\tau). \quad (6)$$

For $\alpha < 0$, the integral in (6) converges to a finite value when N and τ_{\max} tend to infinity. Consequently, \bar{t} is constant for large N ; we have $t \sim N$ and the asymptotic behavior of the diffusion process is not changed by the distribution of waiting times, i.e., $\bar{d}_w = d_w$.

In contrast, in the range $0 < \alpha < 1$, \bar{t} diverges as $\bar{t} \sim \tau_{\max}^\alpha$ for τ_{\max} going to infinity, and the diffusion exponent is changed. To see how τ_{\max} depends on S (and N) let us consider first how the waiting times τ are chosen from random numbers x , $0 < x < 1$. Since the random numbers x are homogeneously distributed, we have $P(\tau)d\tau = dx$. This yields $\tau \sim x^{1/(\alpha-1)}$. Now consider S random numbers x . The minimum value of the S numbers scales as $x_{\min} \sim 1/S$. Accordingly, the maximum value τ_{\max} chosen from the distribution (2) scales as

$$\tau_{\max} \sim x_{\min}^{1/(\alpha-1)} \sim S^{-1/(\alpha-1)}$$

and we obtain from (6)

$$\bar{t} \sim S^{\alpha/(1-\alpha)}. \quad (7)$$

Taking into account that $S \sim N^{d_s/2}$ for $d_s \leq 2$ and $S \sim N$ for $d_s > 2$, where d_s is the fracton dimension^{6,16} (6), we obtain

$$t = N\bar{t} \sim \begin{cases} N^{d_s \alpha / [2(1-\alpha)] + 1}, & d_s < 2 \\ N^{\alpha/(1-\alpha) + 1}, & d_s \geq 2. \end{cases} \quad (8)$$

Using (5) we get

$$\langle r^2 \rangle \sim t^{2/\bar{d}_w},$$

where

$$\bar{d}_w = \begin{cases} d_w, & -\infty < \alpha \leq 0 \\ d_w \left[1 + \frac{d_s}{2} \frac{\alpha}{1-\alpha} \right], & 0 < \alpha < 1, d_s < 2 \\ d_w / (1-\alpha), & 0 < \alpha < 1, d_s \geq 2. \end{cases} \quad (9)$$

Equation (9) is the basic result of the paper and holds for Euclidean lattices as well as for fractal structures. For Euclidean lattices in two and higher dimensions one has $d_s \geq 2$, $d_w = 2$ (Refs. 6 and 16), and (9) reduces to the conventional result $\bar{d}_w = 2/(1-\alpha)$.⁸ In one dimension,

$d_s = 1$, and (9) yields again the exact result $\bar{d}_w = (2-\alpha)/(1-\alpha)$, $0 \leq \alpha < 1$.⁷ For fractal structures one has⁶ $d_s = 2d_f/d_w$ and (9) becomes

$$\bar{d}_w = \begin{cases} d_w, & -\infty < \alpha < 0 \\ d_w + d_f \frac{\alpha}{1-\alpha}, & 0 \leq \alpha < 1. \end{cases} \quad (10)$$

For the Sierpinski gasket and the Van-Koch curve, (10) reduces to a result, which has been recently derived by Robillard and Tremblay¹³ using a renormalization-group approach. But since our scaling arguments do not rely on any details of the fractal structure we believe that (10) is valid in general, for deterministic as well as for random fractals. For fractal structures, (10) differs considerably from the result of the continuous-time random-walk approach,¹²

$$\bar{d}_w = \begin{cases} d_w, & -\infty < \alpha \leq 0 \\ d_w / (1-\alpha), & 0 \leq \alpha < 1 \end{cases} \quad (11)$$

which can be thought of as a mean-field approximation where memory effects are neglected. Indeed, above the marginal dimension $d_s = 2$ Eq. (9) reduces to the mean-field result Eq. (11).¹² In (9) and (10), the diffusion exponent sticks at its conventional value d_w for $\alpha < \alpha_c = 0$. The cross over value $\alpha_c = 0$ has a simple physical interpretation. Only for $\alpha < \alpha_c$ there exists a stationary equilibrium distribution

$$P_{(\bar{r})}^{\text{eq}} \equiv \lim_{t \rightarrow \infty} P(\mathbf{r}, t).$$

Detailed balance¹⁷ requires

$$\lim_{S \rightarrow \infty} \frac{1}{S} \sum_{i=1}^S P^{\text{eq}}(\mathbf{r}_i) \sim \bar{t}$$

and hence [see Eqs. (6) and (7)] the stationary distribution function can be normalized only for $\alpha < \alpha_c = 0$. Accordingly, the diffusion exponent \bar{d}_w is only changed by the distribution of waiting times if a stationary equilibrium state does not exist.

In order to check the validity of (10) for random fractals, we have investigated random walks on the incipient percolation cluster in $d=2$. We have performed computer simulations using the exact enumeration method.¹⁸ In this method, the distribution function $P(\mathbf{r}, t)$ of a random walker in a given system is calculated exactly for a fixed starting point \mathbf{r}_0 of the walker. $P(\mathbf{r}, t)$ is defined as the probability of finding the walker in a distance \mathbf{r} from its starting point \mathbf{r}_0 at time t .

First, using the Leath algorithm,¹⁹ we generated a percolation cluster on a square lattice at criticality starting from the origin $\mathbf{r}_0 = 0$. The transition rates w_r from each site \mathbf{r} to one of its neighboring cluster sites are chosen according to

$$w_r = \frac{1}{4} R^{1/(1-\alpha)}, \quad (12)$$

where R is a random number between 0 and 1. By this procedure we generated a distribution of waiting times according to Eq. (2). The time evolution of $P(\mathbf{r}, t)$ was calculated as follows. At time $t=0$ the walker starts in the

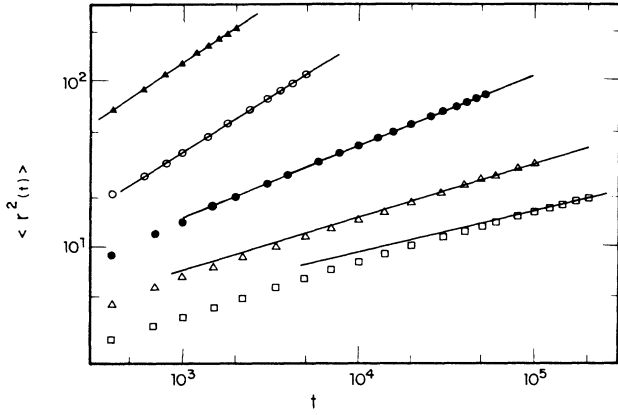


FIG. 1. Plot of $\langle r^2(t) \rangle$ vs time t for various values of α obtained from our computer simulations. The solid lines have the slope displayed in Table I. ▲: $\alpha = -\infty$; ●: $\alpha = \frac{1}{2}$; □: $\alpha = \frac{3}{4}$; ○: $\alpha = 0$; △: $\alpha = \frac{2}{3}$.

origin, i.e., $P(\mathbf{r}, 0) = \delta_{\mathbf{r}, 0}$. At time $t=1$, the walker steps with probability w_0 to each of his neighboring cluster sites δ . Therefore

$$P(\mathbf{r}, 1) = \begin{cases} w_0, & \mathbf{r} = \delta \\ 1 - \sum_{\delta} w_0, & \mathbf{r} = 0 \\ 0, & \text{else} \end{cases}$$

By iterating this procedure we find $P(\mathbf{r}, 2)$, etc. From $P(\mathbf{r}, t)$ we obtain the mean-square displacement

$$\langle r^2(t) \rangle = \sum_{\mathbf{r}} r^2 P(\mathbf{r}, t) \quad (13)$$

of the random walker with starting point at the origin for the given cluster. In order to obtain the corresponding configurational averaged quantity we have to average over many clusters. Another interesting quantity is the probability $\tilde{P}(l, t)$ to find the walker in a chemical distance l from his starting point. The chemical distance l between two points in the cluster is defined as length of the short-

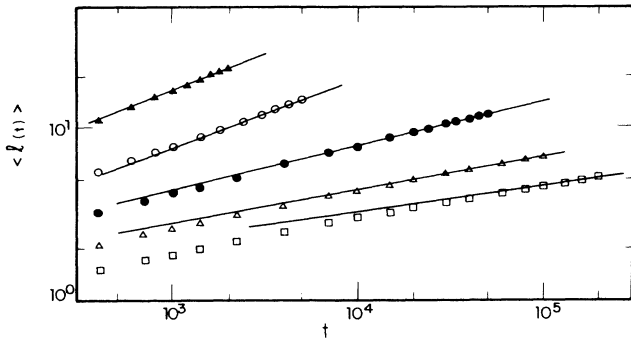


FIG. 2. Plot of $\langle l(t) \rangle$ vs time t for various values of α . The solid lines have the slope displayed in Table I. ▲: $\alpha = -\infty$; ●: $\alpha = \frac{1}{2}$; □: $\alpha = \frac{3}{4}$; ○: $\alpha = 0$; △: $\alpha = \frac{2}{3}$.

TABLE I. The diffusion exponents \bar{d}_w and \bar{d}_w^l extracted from Figs. 1 and 2, compared with the theoretical prediction, Eq. (10).

α	Numerical \bar{d}_w	Numerical \bar{d}_w^l	Numerical \bar{d}_w^l / \bar{d}_w	Theory \bar{d}_w
$-\infty$	2.83 ± 0.1	2.4 ± 0.1	0.85	2.87
0	3.0 ± 0.2	2.5 ± 0.2	0.83	2.87
$\frac{1}{2}$	4.7 ± 0.2	4.0 ± 0.2	0.85	4.76
$\frac{2}{3}$	6.2 ± 0.6	5.2 ± 0.5	0.84	6.66
$\frac{3}{4}$	8.0 ± 0.8	6.6 ± 0.6	0.82	8.56

test path between them.²⁰ To each cluster site \mathbf{r} a chemical distance l is attributed. Consequently, $P(\mathbf{r}, t)$ and $\tilde{P}(l, t)$ are related by

$$\tilde{P}(l, t) = \sum_{\mathbf{r}}^{(l)} P(\mathbf{r}, t), \quad (14)$$

where $\sum_{\mathbf{r}}^{(l)}$ denotes a sum over all sites with the same chemical distance l from the origin. From $\tilde{P}(l, t)$ one can calculate the mean chemical distance $\langle l(t) \rangle$

$$\langle l(t) \rangle = \sum_l l \tilde{P}(l, t) \quad (15)$$

the walker travelled at time t . The asymptotic behavior of $\langle l \rangle$ is described by the exponent \bar{d}_w^l ,

$$\langle l(t) \rangle \sim t^{1/\bar{d}_w^l}. \quad (16)$$

For constant waiting times we define $\langle l \rangle \sim t^{1/d_w^l}$. It is known that $d_w^l \simeq 0.88 d_w$ (Ref. 20) for $d=2$ percolation. Analogous to (5) we have generally $\langle l \rangle \sim N^{1/d_w^l}$. Substituting this result into (8) we find

$$\frac{\bar{d}_w^l}{\bar{d}_w} = \frac{d_w^l}{d_w} \simeq 0.88, \quad (17)$$

irrespective of the waiting time exponent α . Eq. (17) can serve as useful test of numerical calculations.

For our actual computations we have generated clusters of up to 120 shells and averaged $\langle r^2 \rangle$ and $\langle l \rangle$ for each value of α , over 400 clusters. The results for $\langle r^2 \rangle$ and $\langle l \rangle$ as function of time for $\alpha = -\infty, 0, \frac{1}{2}, \frac{2}{3}$, and $\frac{3}{4}$ are shown in Figs. 1 and 2. For $\alpha = \frac{2}{3}$ and $\frac{3}{4}$ the asymptotic regime was not yet reached. Here we obtained the transport exponents \bar{d}_w and \bar{d}_w^l by calculating the successive slopes of the curves as function of $1/t$ and by extrapolating the results to $1/t=0$. The numerical results for the exponents are compared with our theoretical predictions in Table I. The agreement between theory and simulation is very good.

III. DISTRIBUTION FUNCTIONS AND MOMENTS

Next we are interested in the distribution functions $P(\mathbf{r}, t)$ and $\tilde{P}(l, t)$. Following suggestions of Havlin *et al.*¹⁵ for constant waiting times we write analogously

$$P(\mathbf{r}, t) \sim t^{-d_f/\bar{d}_w} r^{d_f-1} e^{-a(r/t)^{1/\bar{d}_w}}, \quad (18a)$$

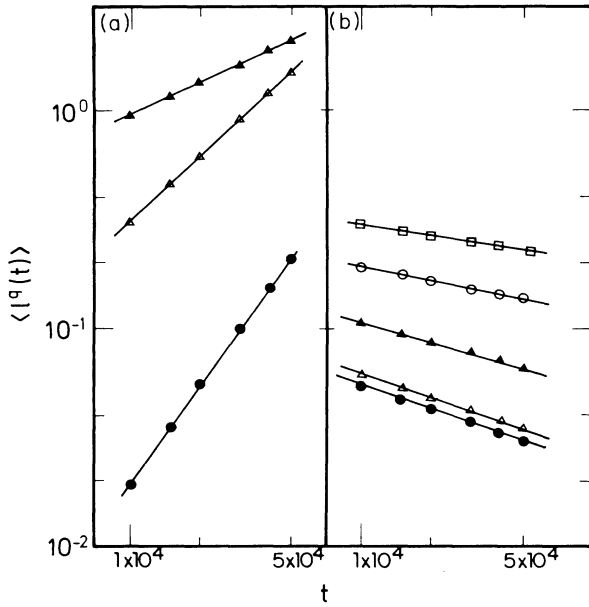


FIG. 3. Numerical results for $\langle l^q(t) \rangle$ as a function of t for $\alpha = \frac{1}{2}$ and different values of q . In order to show the data points for different values of q in one figure, we have multiplied the results for $\langle l^q(t) \rangle$ in (a) for each value of q by an appropriate factor C . (a) \blacktriangle : $q=2, C=10^{-2}$; \triangle : $q=4, C=10^{-5}$; \bullet : $q=6, C=10^{-9}$. (b) \square : $q=-0.8$; \circ : $q=-1.2$; \blacktriangle : $q=-2$; \triangle : $q=-4$; \bullet : $q=-6$.

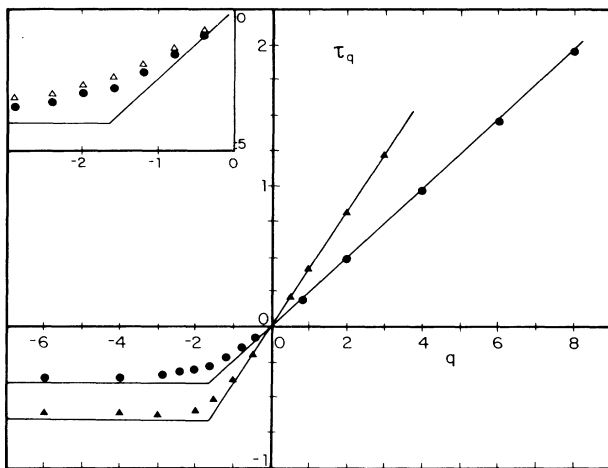


FIG. 4. Plot of τ_q as a function of q for $\alpha = -\infty$ (\blacktriangle) and $\alpha = \frac{1}{2}$ (\bullet). For $\alpha = -\infty$, the slope τ_q has been measured in the vicinity of time $t=2000$; for $\alpha = 1/2$, τ_q has been measured near $t=50000$. The solid lines are our theoretical predictions, Eqs. (22) and (23). The inset shows τ_q for $\alpha = \frac{1}{2}$ measured in the vicinity of $t=25000$ (\triangle) and $t=50000$ (\bullet).

$$\bar{P}(l,t) \sim t^{-d_f/\bar{d}_w} l^{d_f-1} e^{-b(l/t)^{1/\bar{d}_w} \delta}, \quad (18b)$$

where d_f and d_l are the fractal and the chemical fractal dimension²⁰ of the percolation cluster; a and b are constants. Concerning the exponents γ and δ there is not much known up to know and we will come back to this point later. From now on we will mainly concentrate on $\bar{P}(l,t)$ since, as mentioned before, it contains the same information about the dynamical properties of the system as $P(r,t)$. From the distribution one can calculate all its moments $\langle l^q(t) \rangle$ via

$$\langle l^q(t) \rangle = \sum_{l=1}^{\infty} l^q \bar{P}(l,t). \quad (19)$$

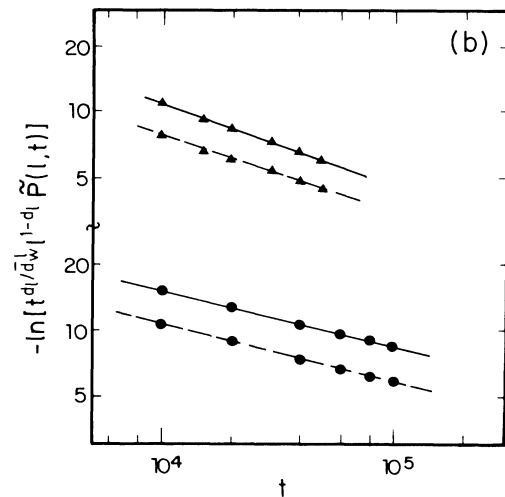
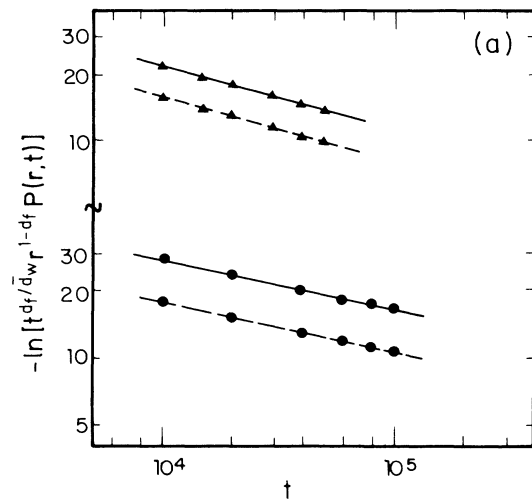


FIG. 5. (a) Plot of $-\ln[t^{d_f/\bar{d}_w} r^{1-d_f} P(r,t)]$ vs time t for $\alpha = \frac{1}{2}$, $r=50$ (\blacktriangle : solid line), $\alpha = \frac{1}{2}$, $r=40$ (\triangle : dashed line), $\alpha = \frac{2}{3}$, $r=40$ (\bullet : solid line) and $\alpha = \frac{2}{3}$, $r=30$ (\bullet : dashed line). (b) Plot of $-\ln[t^{d_l/\bar{d}_w} l^{1-d_l} \bar{P}(l,t)]$ vs time t for $\alpha = \frac{1}{2}$, $l=50$ (\blacktriangle : solid line), $\alpha = \frac{1}{2}$, $l=40$ (\triangle : dashed line), $\alpha = \frac{2}{3}$, $l=40$ (\bullet : solid line), $\alpha = \frac{2}{3}$, $l=30$ (\bullet : dashed line).

The time dependence of each moment is described by an exponent τ_q

$$\langle l^q(t) \rangle \sim t^{\tau_q} . \quad (20)$$

Assuming $\bar{P}(l, t)$ to have the form (18b) the moments can be written as

$$\langle l^q(t) \rangle \sim t^{q/\bar{d}_w^l} \int_{t^{-1/\bar{d}_w^l}}^{\infty} dx x^{d_l+q-1} e^{-bx^\delta} . \quad (21)$$

with $x = l/t^{1/\bar{d}_w^l}$. For t going to infinity the lower bound of the integral tends to zero. For $q > -d_l$, the upper limit of the integral is dominant and we find

$$\tau_q = q/\bar{d}_w^l, \quad q \geq -d_l . \quad (22)$$

In contrast, for $q < -d_l$ the lower limit contributes to the integral and we obtain

$$\tau_q = -d_l/\bar{d}_w^l, \quad q < -d_l . \quad (23)$$

To check these predictions, we have calculated the moments $\langle l^q(t) \rangle$ for several values of α and many values of q by the exact enumeration method. Figure 3 shows the results for a representative value of α , $\alpha = \frac{1}{2}$, and a few values of q . From the slopes of these curves we obtain the exponents τ_q . In Fig. 4 the numerical results for the exponents τ_q as a function of q for $\alpha = -\infty$ and $\alpha = \frac{1}{2}$ are compared with the theoretical predictions Eqs. (22) and (23). For $q \lesssim -3$ and $q \gtrsim -1$ the theory fits very well the numerical data, only the crossover in the vicinity of $q = -d_l$ is smeared out in the numerical results. As can be seen from the inset of Fig. 4, this effect decreases when t is increased. Therefore, we believe that in the long-time limit our numerical data will converge towards a sharp cross over as predicted theoretically; however our numerical data cannot exclude the case that this smeared cross over may remain for large t which would cause the distribution to be of multifractal nature.

Finally we consider the exponents γ and δ which appear in the distribution functions, Eqs. (18). It was suggested by several authors^{21,22} that $\gamma = d_w$ and $\delta = d_w^l$ and by others^{23,15} that γ is related to d_w by

$$\gamma = \frac{d_w}{d_w - 1} \quad (24a)$$

which directly leads to¹⁵

$$\delta = \frac{d_w^l}{d_w^l - 1} . \quad (24b)$$

From numerical studies for constant waiting times it has been proposed¹⁵ that (24) is not rigorous but the correct values of the exponents are somewhat higher. To determine γ and δ for $\alpha = \frac{1}{2}$ and $\frac{2}{3}$ we have plotted in Fig. 5

$$-\ln[t^{d_f/\bar{d}_w} r^{1-d_f} P(r, t)]$$

as a function of t for two different values of r and

$$-\ln[t^{d_l/\bar{d}_w^l} l^{1-d_l} \bar{P}(l, t)]$$

as a function of t for two values of l . Our numerical data follow very accurately straight lines. The slopes determine γ and δ . We find

$$\gamma = 1.4 \pm 0.15 \left[\frac{\bar{d}_w}{\bar{d}_w - 1} = 1.27 \pm 0.02 \right]$$

and

$$\delta = 1.43 \pm 0.15 \left[\frac{\bar{d}_w^l}{\bar{d}_w^l - 1} = 1.33 \pm 0.03 \right]$$

for $\alpha = \frac{1}{2}$ and $\gamma = 1.25 \pm 0.15$ (1.2 ± 0.03) and $\delta = 1.37 \pm 0.15$ (1.24 ± 0.04) for $\alpha = \frac{2}{3}$. Accordingly, our numerical values for γ and δ are considerably smaller than \bar{d}_w and \bar{d}_w^l , and somewhat larger than those predicted by (24) which seems to support the conclusion of former numerical studies.¹⁵ However, the errorbars of our results are too large to exclude the validity of (24).

ACKNOWLEDGMENTS

The authors wish to thank W. Dieterich, D. Stauffer, and H. Weissman for helpful discussions. This work has been supported by Deutsche Forschungsgemeinschaft (in particular, Sonderforschungsbereich 306), Minerva, and the USA-Israel Binational Foundation.

¹R. Orbach, *Science* **231**, 814 (1986).

²D. Stauffer, *Introduction to Percolation Theory* (Taylor and Francis, London, 1985).

³*Scaling Phenomena in Disordered Systems*, edited by R. Pynn and A. Skjeltorp (Plenum, New York, 1985).

⁴A. Bunde, *Adv. Solid State Phys.* **26**, 113 (1986).

⁵S. Havlin and D. Ben-Avraham, *Adv. Phys.* (to be published).

⁶S. Alexander and R. Orbach, *J. Phys. (Paris) Lett.* **43**, L625 (1982); Y. Gefen, A. Aharony, and S. Alexander, *Phys. Rev. Lett.* **50**, 77 (1983).

⁷S. Alexander, J. Bernasconi, W. R. Schneider, and R. Orbach, *Rev. Mod. Phys.* **53**, 175 (1981).

⁸S. Alexander, *Phys. Rev. B* **23**, 2951 (1981).

⁹B. I. Halperin, S. Feng, and P. N. Sen, *Phys. Rev. Lett.* **54**, 2391 (1985); S. Feng, B. I. Halperin, and P. N. Sen, *Phys. Rev. B* **35**, 197 (1987).

¹⁰M. Kogut and J. P. Straley, *J. Phys. C* **12**, 2151 (1979).

¹¹A. Bunde, H. Harder, and S. Havlin, *Phys. Rev. B* **34**, 3540 (1986).

¹²A. Blumen, J. Klafter, B. S. White, and G. Zumofen, *Phys. Rev. Lett.* **53**, 1301 (1984).

¹³S. Robillard, and A.-M.S. Tremblay, *J. Phys. A* **19**, 2171 (1986).

¹⁴S. Havlin, B. Trus, and G. H. Weiss, *J. Phys. A* **19**, L817 (1986).

¹⁵S. Havlin, D. Movshovitz, B. Trus, and G. H. Weiss, *J. Phys.*

- A **18**, L719 (1985).
- ¹⁶S. Alexander, *Physica* **140A**, 397 (1986).
- ¹⁷H. Scher, and M. Lax, *Phys. Rev. B* **7**, 4491 (1973).
- ¹⁸I. Majid, D. Ben-Avraham, S. Havlin, and H. E. Stanley, *Phys. Rev. B* **30**, 1626 (1984).
- ¹⁹P. L. Leath, *Phys. Rev. B* **14**, 5046 (1976).
- ²⁰S. Havlin and R. Nossal, *J. Phys. A* **17**, L427 (1984).
- ²¹B. O'Shaughnessy and I. Procaccia, *Phys. Rev. Lett.* **54**, 344 (1985); *Phys. Rev.* **32**, 3073 (1985).
- ²²J. R. Banavar and J. Williamson, *Phys. Rev. B* **30**, 6778 (1984).
- ²³R. A. Guyer, *Phys. Rev. A* **29**, 2751 (1984).